

## Antidot density dependence of magnetization reversal dynamics in ultrathin epitaxial Fe/GaAs(001)

This article has been downloaded from IOPscience. Please scroll down to see the full text article.

2004 J. Phys.: Condens. Matter 16 L375

(<http://iopscience.iop.org/0953-8984/16/32/L01>)

View [the table of contents for this issue](#), or go to the [journal homepage](#) for more

Download details:

IP Address: 150.178.12.75

The article was downloaded on 24/06/2013 at 14:58

Please note that [terms and conditions apply](#).

## LETTER TO THE EDITOR

## Antidot density dependence of magnetization reversal dynamics in ultrathin epitaxial Fe/GaAs(001)

T A Moore<sup>1</sup>, G Wastlbauer<sup>1</sup>, J A C Bland<sup>1</sup>, E Cambri<sup>2</sup>, M Natali<sup>2</sup>,  
D Decanini<sup>2</sup> and Y Chen<sup>2</sup>

<sup>1</sup> Cavendish Laboratory, University of Cambridge, Cambridge, CB3 0HE, UK

<sup>2</sup> Laboratoire de Photonique et de Nanostructures, CNRS, Route de Nozay, 91460 Marcoussis, France

E-mail: jacb1@phy.cam.ac.uk

Received 2 April 2004

Published 30 July 2004

Online at [stacks.iop.org/JPhysCM/16/L375](http://stacks.iop.org/JPhysCM/16/L375)

doi:10.1088/0953-8984/16/32/L01

### Abstract

Easy axis dynamic magneto-optic Kerr effect loops have been measured from ultrathin (2 nm) epitaxial Fe/GaAs(001) films patterned with arrays of 1  $\mu\text{m}$  square antidots of different densities (antidot spacings 10–50  $\mu\text{m}$ ). The applied field was sinusoidal with frequency  $f = 0.01 \text{ Hz} - 2.3 \text{ kHz}$ . A study of dynamic coercivity  $H_c^*$  as a function of  $f$  reveals an intermediate dynamic regime ( $20 \text{ Hz} < f < 1000 \text{ Hz}$ ) characterized by a dip in  $H_c^*$  that is suppressed at high antidot density. The dip is attributed to timescale matching of the sweeping applied field with the domain wall propagation in the film. Suppression of the dip is explained by an increase of domain nucleation in the higher antidot density films in the intermediate dynamic regime.

As part of the drive to understand and control fast switching in magnetic materials, the study of thin film magnetization reversal dynamics remains of considerable fundamental and technological importance. Continuous thin magnetic films reverse via domain nucleation and wall propagation, and the timescales on which these processes occur are understood to depend on temperature, magnetic anisotropy strength, Barkhausen volume and applied field strength and sweep rate [1, 2]. An effective method to probe reversal dynamics in thin magnetic films is to measure dynamic hysteresis loops by means of the *ac* magneto-optic Kerr effect and to examine the field sweep rate dependence of the dynamic coercivity. Recent experimental and theoretical studies have shown that there are two distinct regimes in the variation of dynamic coercivity with field sweep rate, corresponding to a change in the principal reversal mechanism from domain wall propagation at low sweep rate to domain nucleation at high sweep rate [3, 4]. In epitaxial Fe/GaAs(001), at the crossover between these two regimes, the dynamic coercivity has been found to dip, and this has been explained to be the result of competition between

the wall propagation and nucleation processes [2]. To test for such a competition, in this work the relative contributions of wall propagation and nucleation to the reversal of ultrathin epitaxial Fe/GaAs(001) are controlled and the effect on the sweep-rate-dependent coercivity (and on the dip in the coercivity at the crossover between dynamic regimes) is measured. Arrays of artificially produced holes (antidots) are used to control the domain processes. The modified energy landscape at antidot sites not only hinders domain wall movement [5], but also influences domain nucleation [6].

An ultrathin (2 nm) continuous epitaxial Fe film was prepared on GaAs(001) by molecular beam epitaxy at ambient temperature (35 °C) in ultrahigh vacuum. The film was patterned with three antidot arrays, each of overall size 0.5 mm × 0.5 mm and with different antidot spacings  $s = 10, 20$  and  $50 \mu\text{m}$ . The antidots were  $1 \mu\text{m}$  square holes through the Fe and protective Au (3 nm) layers down to the top surface of the GaAs. Patterning was done in three stages: (i) electron beam lithography on PMMA resist (400 nm), (ii) etching by argon ion beam (200 eV), (iii) removal of PMMA in trichloroethylene. A region of continuous film was left as a reference.

Dynamic hysteresis ( $M$ – $H$ ) loops were measured using a Kerr magnetometer, with a time-varying magnetic field  $H(t) = H_0 \sin(2\pi ft)$  applied in plane and along the uniaxial easy axis [110]. In epitaxial Fe/GaAs(001) a surface-induced uniaxial anisotropy arises which is thickness dependent and dominates over the bulklike magnetocrystalline cubic anisotropy up to  $\sim 5$  nm coverage [7]. The field frequency  $f$  was varied from 0.01 Hz to 2.3 kHz, and the field amplitude  $H_0$  was maintained at 120 Oe, sufficient to saturate the magnetization along [110] for all frequencies. For  $f < 10$  Hz hysteresis loops were captured after one field cycle, whilst for  $f \geq 10$  Hz the hysteresis loops were recorded after several hundred field cycles. The photodetector (response time  $\sim 30$  ns) and Hall probe (response time  $\sim 3 \mu\text{s}$ ) signals,  $M(t)$  and  $H(t)$  respectively, were captured on a 400 MHz bandwidth oscilloscope.

It has been previously reported that, in sufficiently low frequency applied fields, ultrathin epitaxial Fe/GaAs(001) films reverse via the propagation of  $180^\circ$  domain walls between interface pinning sites [4]. The goal of the present experiment was to control domain wall pinning by varying the antidot density, and to investigate the effect on the reversal process of extending the applied field frequency into the kilohertz regime. The antidots can be expected to act as artificial pinning sites, and their separations were chosen to be less than  $100 \mu\text{m}$  in order that their effect on pinning would dominate that of intrinsic interface pinning sites (separation  $\sim$  few hundred micrometres [4]), yet not so small that the reversal mechanism would be radically altered.

Representative dynamic hysteresis loops are shown in figure 1 for the patterned 2 nm Fe/GaAs(001), antidot spacings  $s = 10, 20$  and  $50 \mu\text{m}$ , and for the continuous film. For  $s = 10$  and  $20 \mu\text{m}$ , the coercive field at 100 Hz is approximately 5% and 11% larger than that at 10 Hz, respectively. For  $s = 50 \mu\text{m}$  and for the continuous film the coercive field decreases by approximately 16% and 8% respectively with increasing frequency in the range 10–100 Hz. The loops are very square, especially for  $s = 20$  and  $50 \mu\text{m}$ , and for the continuous film, as expected for the uniaxial easy axis orientation. For  $s = 10 \mu\text{m}$  the slope at the coercive field changes with increasing frequency from 10 to 100 Hz, indicating that the switching field distribution becomes more widely spread. It is likely that the higher density of antidots here increases the switching field distribution via increased domain wall pinning.

Values of the dynamic coercive field  $H_c^*$  (coercive field measured from a dynamic hysteresis loop) were extracted from the loops and plotted as a function of frequency (figure 2). There are three distinct regions in these data, marked by dashed lines in the figure. First, there is the low dynamic regime ( $f < 20$  Hz), where the dynamic coercive field is a linear function of the logarithm of applied field frequency, the gradient being determined by an interface

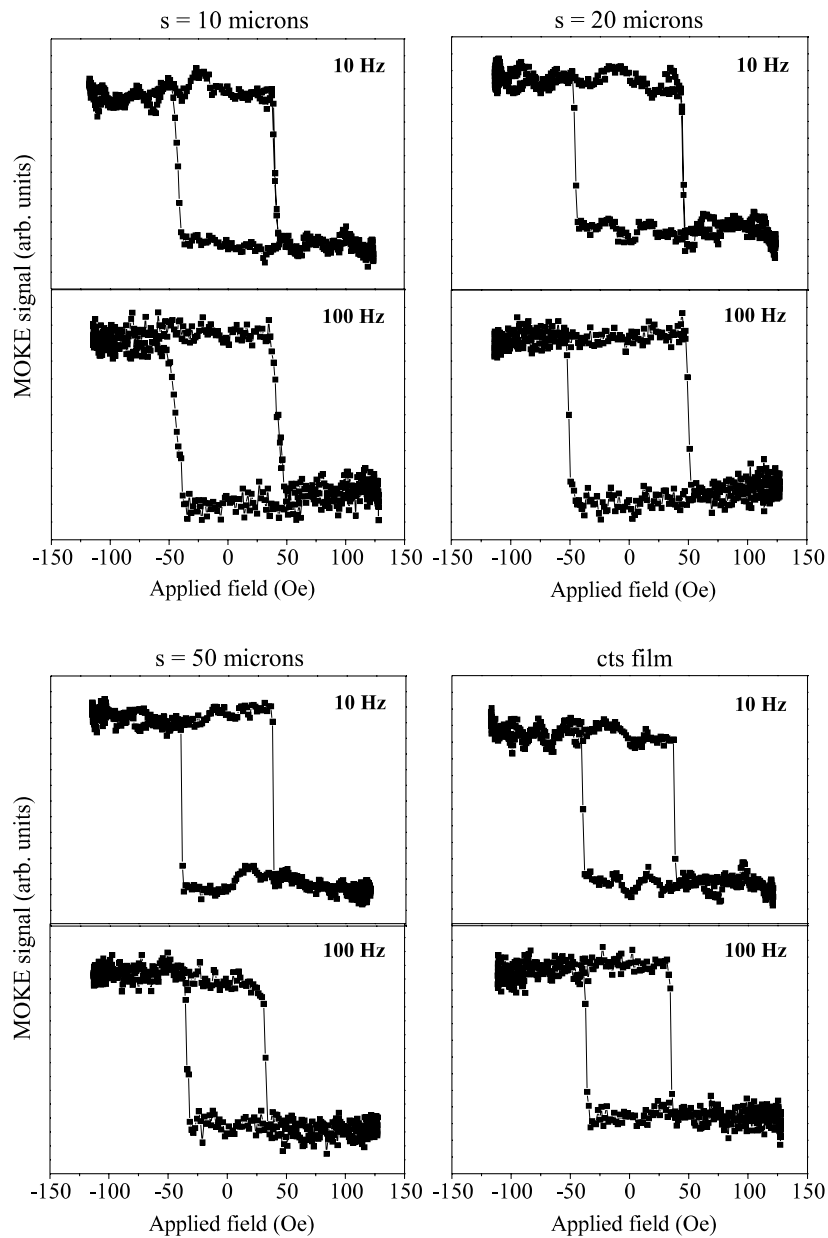


**Figure 1.** Representative dynamic hysteresis loops for the patterned 2 nm Fe/GaAs(001) for field applied along the uniaxial easy axis, antidot spacings  $s = 10, 20$  and  $50 \mu\text{m}$ , and for the continuous ('cts') film.

pinning effect [8]. Here, reversal is predominantly by domain wall motion. Second, there is an intermediate dynamic regime ( $20 \text{ Hz} < f < 1000 \text{ Hz}$ ), which, depending on the antidot density, may be characterized by a dip in the  $H_c^* - f$  data. At low antidot density (i.e. in the continuous film, and for  $s = 50 \mu\text{m}$ ) the dynamic coercivity decreases ('dips') with increasing frequency in the intermediate dynamic regime, whilst for higher antidot density ( $s = 20$ ,

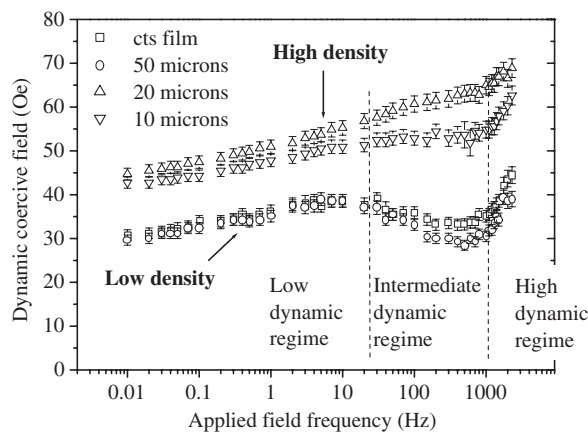


**Figure 2.** Dynamic coercive field  $H_c^*$  as a function of applied field frequency  $f$  for the patterned 2 nm Fe/GaAs(001), antidot spacings  $s = 10, 20$  and  $50 \mu\text{m}$ , and for the continuous ('cts') film. The data for  $s = 10$  and  $20 \mu\text{m}$  are shifted by  $+10$  Oe, in order to highlight the different trends in dynamic coercive field for high and low antidot density samples.

$10 \mu\text{m}$ ) the dynamic coercivity remains almost a constant, or increases. In the intermediate dynamic regime, domain nucleation as well as wall motion contributes to the magnetization reversal. Finally, there is a high dynamic regime ( $f > 1000$  Hz) where the dynamic coercivity climbs quickly as a function of frequency. Here, domain nucleation plays a dominant role in the reversal.

The key feature of the data in figure 2 is that the dip in coercivity is suppressed at higher antidot density. Assuming that antidots pin domain walls, one can expect that the greater the antidot density, the slower the wall motion. Conversely, where there are fewer antidots one can expect the domain walls to move more freely. It is in the latter case that the dip in coercivity is seen, and it can be considered to occur when the applied field is swept fast enough that domain walls are forcibly depinned from their nucleation sites and driven through the film by the field. In this situation the magnetization reversal begins at a lower field value and completes more quickly than at lower applied field frequency, thus the coercivity is seen to decrease with increasing frequency (into the dip). In the case of high antidot density the wall motion is hindered, and although the reversal may begin at a lower field value, it cannot complete quickly and therefore the dip in dynamic coercivity is suppressed.

The fact that  $H_c^*$  for  $s = 10 \mu\text{m}$  is consistently smaller than that for  $s = 20 \mu\text{m}$  can be considered an indicator of competition between wall propagation and domain nucleation mechanisms. If the antidots act as nucleation centres (promoting reversal by domain nucleation) as well as wall pinning sites (hindering reversal by wall propagation), then there will be an optimum antidot density for maximum coercive field at a given frequency. If the antidot density is higher than this optimum, domain nucleation will be encouraged and the coercive field will fall. On the other hand, if the antidot density is lower, wall propagation is easier and the coercive field also falls. In this 2 nm Fe/GaAs(001) film  $s = 20 \mu\text{m}$  gives the maximum coercive field.

In a separate study [2] of sweep-rate-dependent switching in 15 nm continuous epitaxial Fe/GaAs(001), a dip in dynamic coercivity at the transition from the low to the high dynamic regime was reported. The existence of the dip implied that there were two timescales associated with the reversal process, and it was assumed that these corresponded to domain nucleation and wall motion, respectively. Importantly, the 'propagation time' ( $\tau_p$ , which includes both wall

**Table 1.** Timescales  $\tau_n$  (nucleation) and  $\tau_p$  (propagation) for square antidot arrays of spacing  $s$  on 2 nm Fe/GaAs(001).

| $s$ ( $\mu\text{m}$ ) | $\tau_n$ ( $\mu\text{s}$ ) | $\tau_p$ ( $\mu\text{s}$ ) | $\tau_n/\tau_p$ |
|-----------------------|----------------------------|----------------------------|-----------------|
| 10                    | $31 \pm 3$                 | $48 \pm 5$                 | $0.65 \pm 0.09$ |
| 20                    | $33 \pm 26$                | $36 \pm 31$                | $0.92 \pm 1.07$ |
| 50                    | $94 \pm 12$                | $270 \pm 32$               | $0.35 \pm 0.06$ |
| 1000                  | $73 \pm 10$                | $162 \pm 21$               | $0.45 \pm 0.09$ |

depinning and motion between pinning sites) controlled the onset of the dip, and the ‘nucleation time’ ( $\tau_n$ ) controlled the onset of the high dynamic regime. Here, a similar empirical expression to fit to the antidot density-dependent data is used, but with an extra term to allow for the slope in the low dynamic regime:

$$H_c^* = H_{c, P \rightarrow 0}^* \exp\left(\frac{-P}{P_n}\right) + H_c \left(1 - \exp\left(\frac{-P}{P_p}\right)\right) - H_b \ln(P). \quad (1)$$

This expression uses the idea of competing domain wall motion and nucleation processes at the transition from the low to the high dynamic regime, as proposed by Raquet *et al* [3].  $P$  is the drive field period, and  $P_n$  and  $P_p$  are the critical field periods for nucleation and propagation, respectively. The critical periods correspond to those frequencies where the field begins to be swept fast enough through the coercive field  $H_c$  that it changes significantly on the appropriate ‘intrinsic’ timescale  $\tau_n$  or  $\tau_p$ . This can be considered as ‘timescale matching’ between the sweeping applied field and the nucleation or propagation process. The first term becomes important as  $P$  approaches the same order of magnitude as  $P_n$ , and fits the upturn of  $H_c^*$  in the high dynamic regime. Here, the field increases before nucleation has completed and before there is any large change in magnetization, leading to an increase in dynamic coercivity.  $H_{c, P \rightarrow 0}^*$  is the value to which  $H_c^*$  tends as  $P$  tends to zero. The second term becomes important as  $P$  approaches the same order of magnitude as  $P_p$ , and fits the dip in  $H_c^*$ . Here, the field increases on the timescale for wall propagation, forcibly depinning and driving domain walls, leading to a reduction in dynamic coercivity in the intermediate dynamic regime. The third term dominates at high  $P$  and is needed in order to fit to  $H_c^*$  in the low dynamic regime, which has a logarithmic dependence on field frequency as seen in figure 2.  $H_b$  is proposed as a characteristic field barrier to reversal associated with an interface-induced domain wall pinning mechanism [8]. Although the third term tends very slowly towards positive (negative) infinity as  $P$  tends to zero (infinity), in the range of  $P$  covered by the experiment these extremes are avoided and the effect on the fit parameters  $P_n$ ,  $P_p$ ,  $H_{c, P \rightarrow 0}^*$ ,  $H_c$  and  $H_b$  is negligible.

Fitting expression (1) to the data in figure 2, and using the method outlined in [2], the timescales  $\tau_n$  and  $\tau_p$  were found, and are shown in table 1 as a function of antidot spacing  $s$ . The continuous film is treated as part of an antidot array that has spacing  $s = 1000 \mu\text{m}$ , since its structure is unbroken on this lengthscale. The timescales for  $s = 20 \mu\text{m}$  have large uncertainties because here the dip is suppressed and there are no clear low  $\rightarrow$  intermediate and intermediate  $\rightarrow$  high dynamic regime transitions.

The first point to note is the distinct change in the ratio  $\tau_n/\tau_p$  between low antidot density ( $s = 1000 \mu\text{m}$ ,  $s = 50 \mu\text{m}$ ) and high antidot density ( $s = 20 \mu\text{m}$ ,  $s = 10 \mu\text{m}$ ), corresponding to whether or not a dip in dynamic coercivity is seen in the intermediate dynamic regime. For the lower antidot densities,  $\tau_n$  is less than half the value of  $\tau_p$ , and the sweeping applied field matches these timescales at distinctly different frequencies, meaning that the dip in dynamic coercivity is seen. For higher antidot density,  $\tau_n$  and  $\tau_p$  are closer in value, and the sweeping applied field matches them at similar frequencies, hence the dip is not seen. The conclusion

may be drawn that the greater the role played by domain nucleation in the intermediate dynamic regime, the closer the values  $\tau_n$  and  $\tau_p$  become and the more the dip in dynamic coercivity is suppressed.

The other distinct trend in table 1 is that both  $\tau_n$  and  $\tau_p$  tend to increase as the antidot density decreases (increasing  $s$ ). This can be explained by assuming that the antidots act as nucleation sites [6], their demagnetizing field locally reducing the energy barrier and promoting nucleation there. The smaller the antidot density, the longer time ( $\tau_n$ ) it will take on average to nucleate a reverse domain. Moreover, domain walls will have to travel further to the next nucleation site in order to complete the reversal, giving a longer  $\tau_p$ .

In this work it has been shown that different antidot densities in an epitaxial 2 nm Fe/GaAs(001) film result in an unusually large difference in coercivity, but only in a regime of intermediate swept-field frequency corresponding to  $20 \text{ Hz} < f < 1000 \text{ Hz}$ . The coercivity of the lower antidot density films decreases with increasing frequency in this regime whilst that of the higher antidot density films remains almost a constant, or increases. The dip in dynamic coercivity for the lower antidot density is attributed to timescale matching of the sweeping applied field with the domain wall propagation in the film. At low antidot density the wall propagation is more important than domain nucleation in the intermediate dynamic regime. The suppression of the dip in dynamic coercivity at high antidot density is attributed to an increase in the role played by domain nucleation in the dynamic magnetization reversal of the film. This change of mechanism is quantified in terms of intrinsic timescales for nucleation and propagation using an empirical adaptation of an existing model of magnetization reversal dynamics. In summary, this work demonstrates the possibility of controlling the domain reversal processes and thereby tuning the coercivity in a particular dynamic range.

The authors acknowledge the support of EPSRC (UK), the EU ESPRIT LTR program 'MASSDOTS' and the EU TMR network 'SUBMAGDEV'. TAM thanks the Cambridge Philosophical Society and Clare College, Cambridge. GW thanks the Austrian Academy of Sciences, the Wilhelm-Macke-Stipendienprivatstiftung (Austria) and the Cambridge Philosophical Society for support.

## References

- [1] Woodward R C, Lance A M, Street R and Stamps R L 2003 *J. Appl. Phys.* **93** 6567
- [2] Moore T A, Wastlbauer G and Bland J A C 2003 *J. Phys.: Condens. Matter* **15** L407
- [3] Raquet B, Mamy R and Ousset J C 1996 *Phys. Rev. B* **54** 4128
- [4] Lee W Y, Choi B C, Xu Y B and Bland J A C 1999 *Phys. Rev. B* **60** 10216
- [5] Vavassori P, Gubbiotti G, Zangari G, Yu C T, Yin H, Jiang H and Mankey G J 2002 *J. Appl. Phys.* **91** 7992
- [6] Guedes I, Grimsditch M, Metlushko V, Vavassori P, Camley R, Ilic B, Neuzil P and Kumar R 2002 *Phys. Rev. B* **66** 014434
- [7] Gester M, Daboo C, Hicken R J, Gray S J, Ercole A and Bland J A C 1996 *J. Appl. Phys.* **80** 347
- [8] Moore T A, Rothman J, Xu Y B and Bland J A C 2001 *J. Appl. Phys.* **89** 7018